

Inhibition of Cancer-Associated Mutant Isocitrate Dehydrogenases: Synthesis, Structure–Activity Relationship, and Selective Antitumor Activity

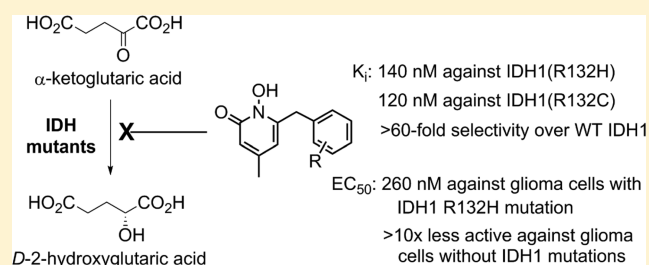
Zhen Liu,^{†,¶} Yuan Yao,^{†,¶} Mari Kogiso,[⊥] Baisong Zheng,[†] Lisheng Deng,[†] Jihui J. Qiu,^{||} Shuo Dong,^{||} Hua Lv,[§] James M. Gallo,[§] Xiao-Nan Li,[⊥] and Yongcheng Song^{*,†,‡,¶}

[†]Department of Pharmacology, [⊥]Department of Pediatrics-oncology, ^{||}Department of Medicine, and [‡]Dan L. Duncan Cancer Center, Baylor College of Medicine, 1 Baylor Plaza, Houston, Texas 77030, United States

[§]Department of Pharmacology and Systems Therapeutics, Icahn School of Medicine at Mount Sinai, One Gustave L. Levy Place, New York, New York 10029, United States

Supporting Information

ABSTRACT: Mutations of isocitrate dehydrogenase 1 (IDH1) are frequently found in certain cancers such as glioma. Different from the wild-type (WT) IDH1, the mutant enzymes catalyze the reduction of α -ketoglutaric acid to D-2-hydroxyglutaric acid (D2HG), leading to cancer initiation. Several 1-hydroxypyridin-2-one compounds were identified to be inhibitors of IDH1(R132H). A total of 61 derivatives were synthesized, and their structure–activity relationships were investigated. Potent IDH1(R132H) inhibitors were identified with K_i values as low as 140 nM, while they possess weak or no activity against WT IDH1. Activities of selected compounds against IDH1(R132C) were found to be correlated with their inhibitory activities against IDH1(R132H), as well as cellular production of D2HG, with R^2 of 0.83 and 0.73, respectively. Several inhibitors were found to be permeable through the blood–brain barrier in a cell-based model assay and exhibit potent and selective activity (EC_{50} = 0.26–1.8 μ M) against glioma cells with the IDH1 R132H mutation.



INTRODUCTION

Isocitrate dehydrogenase (IDH) is one of the key enzymes in the tricarboxylic acid cycle, which provides aerobic organisms the majority of energy by oxidation of the acetyl group derived from, for example, carbohydrates and fats. IDH catalyzes the oxidative decarboxylation of isocitric acid (ICT) to α -ketoglutaric acid (α -KG) using Mg^{2+} and NADP^+ (or NAD^+) as cofactors,¹ as shown in Figure 1A. There are three IDH isozymes in humans, with IDH1 located in cytoplasm and IDH2 and 3 in mitochondria.^{2,3} Moreover, α -KG, the product of the IDH catalyzed reaction, is used as a common cofactor by \sim 60 dioxygenases, including important epigenetic enzymes such as the JmjD family of histone demethylases. Therefore, the function of IDH enzymes is of importance to normal physiology.

Recent genetic studies have identified frequent mutations in IDH genes in several types of cancer.^{4–6} For example, IDH1 mutations are found in \sim 75% of low-grade gliomas (grade II and III), as well as secondary glioblastoma multiforme, the grade IV glioma developed from the low-grade tumors.^{7,8} The R132H mutation is predominant (>90%) in these gliomas. Mutations of IDH1 or IDH2 have also been found in \sim 20% acute myeloid leukemia and many sarcomas.^{6,9–11} The IDH mutations occur at an early stage of these cancers, suggesting they could play important roles in cancer initiation. Of

particular interest is that all characterized IDH mutant proteins, such as IDH1(R132H) and IDH1(R132C), almost lose the catalytic function of wild-type (WT) IDH, but obtain a new capability: they can catalyze the reduction of α -KG to D-2-hydroxyglutaric acid (D2HG) using Mg^{2+} and NADPH as cofactors,^{6,12,13} as shown in Figure 1B. These IDH mutant enzymes therefore cause elevated D2HG concentrations in cell and plasma. Further studies show a high level of D2HG is very harmful and could be the culprit for the initiation of the cancer. Due to its structural similarity to α -KG, D2HG is a broad inhibitor of α -KG-dependent dioxygenases including histone demethylases and the TET-family of 5-methylcytosine hydroxylases,⁵ which are important enzymes keeping a balanced histone and DNA methylation status. Overexpression of IDH1(R132H) can cause hypermethylation of histone and DNA and block cell differentiation.^{14,15} These findings suggest mutant IDH is a novel drug target for intervention,^{16–18} and its inhibitors represent useful probes for the investigation of the biological functions of IDH mutation as well as potential therapeutics for this type of cancer.

A series of diamide compounds, such as compound 1 shown in Figure 1C, were reported to be the first inhibitors of mutant

Received: April 28, 2014

Published: October 1, 2014

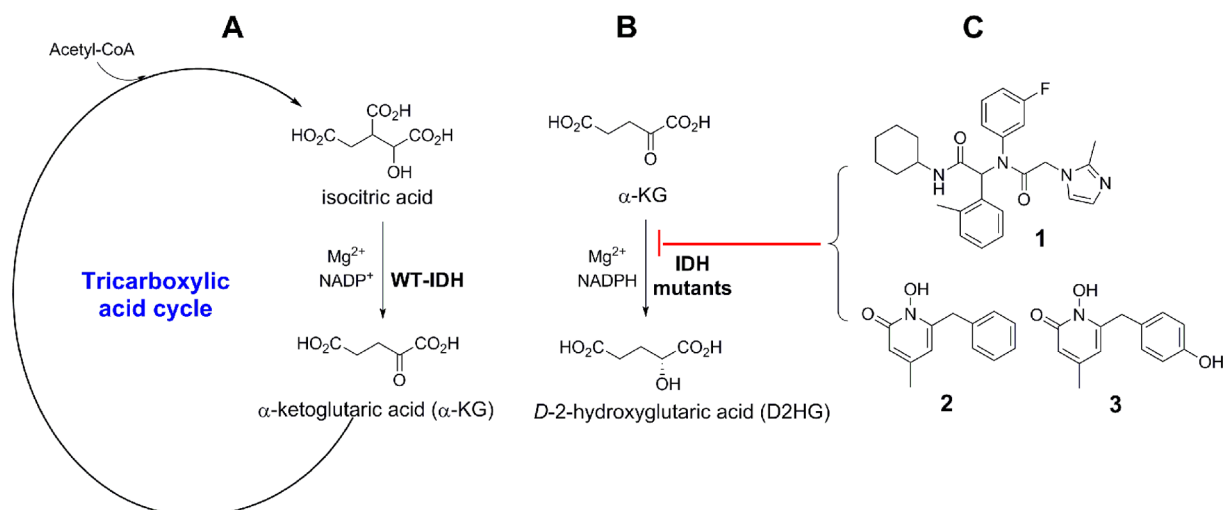


Figure 1. (A) Reaction catalyzed by WT IDH enzymes in tricarboxylic acid cycle, (B) reaction catalyzed by mutant IDH enzymes, and (C) structures of current inhibitors of mutant IDH1.

IDH1 with IC_{50} values as low as 70 nM.^{19,20} Compound 1 is able to reduce the cellular D2HG concentration and slow the proliferation of IDH1 mutated cancer cells. We also reported several 1-hydroxypyridin-2-one compounds,²¹ such as compounds 2 and 3 (Figure 1C), are potent inhibitors of mutant IDH1 with inhibition constant (K_i) values as low as 190 nM, which exhibit very weak activity against WT IDH1 showing a high selectivity of >60-fold. In addition, we determined the X-ray crystal structures of IDH1(R132H) in complex with inhibitors 2 and 3, which reveal the exact binding mode of these two compounds as well as the structural basis for the high selectivity.

Here, we report the inhibitor discovery, design, synthesis, and structure–activity relationships (SAR) of several series of 1-hydroxypyridin-2-one compounds targeting cancer-associated mutant IDH1. Several inhibitors of mutant IDH1 show potent and selective activity against glioma cells with the IDH1 R132H mutation.

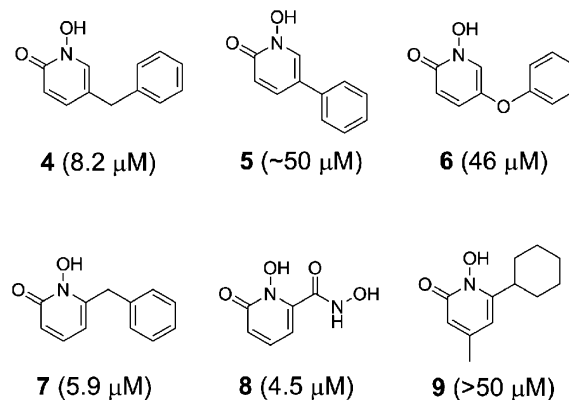
RESULTS AND DISCUSSION

Identification of the Initial Inhibitors of IDH1(R132H).

Our previous research in developing inhibitors of 1-deoxyxylulose-5-phosphate reductoisomerase,^{22–24} another reductase using Mg^{2+} and $NADPH$ as cofactors, provided an enriched source of compounds that could inhibit mutant IDH1. By screening this focused library of ~ 130 compounds against recombinant human IDH1(R132H), the predominant mutation found in the majority of the gliomas, followed by validation, we found several 5- and 6-substituted 1-hydroxypyridin-2-one compounds to be low micromolar inhibitors. The structures and activities of these compounds are shown in Chart 1, together with those of inactive analogs in the library that are useful for SAR analysis.

5-Benzyl-1-hydroxypyridin-2-one (4) was found to be an inhibitor of IDH1(R132H) with a K_i value of 8.2 μM , while compound 5 with a 5-phenyl group has a very weak activity. Compound 6 with an -O- linkage exhibits a K_i of 46 μM , suggesting that an electron-rich core is not favored. Compounds 7 and 8 with a 6-substituent possess an improved activities ($K_i = 5.9$ and 4.5 μM) compared with that of 4. Ciclopirox (9), an antifungal drug, with 4-methyl and 6-cyclohexyl substituents is inactive against IDH1(R132H).

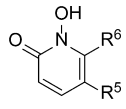
Chart 1. Structures and K_i Values of Initial Inhibitors of IDH1(R132H)



Medicinal Chemistry To Find Potent IDH1(R132H)

Inhibitors. With the identification of 5- and 6-substituted 1-hydroxypyridin-2-one compounds, that is, 4, 7, and 8, as the lead inhibitors of IDH1(R132H), systematic medicinal chemistry studies were performed in an effort to find compounds with improved activity. Four series of compounds, including 5-, 6-, and 4-methyl-6- and 4-methyl-3-substituted 1-hydroxypyridin-2-one compounds, have been designed, synthesized, and tested against IDH1(R132H).

Table 1 shows the structures and activities of 5- or 6-substituted 1-hydroxypyridin-2-one compounds. Compounds 10 and 11, having 5-(2-phenylethyl) and 5-(3-phenylpropyl) substituents, respectively, lose the inhibitory activity. In addition, compounds 12–14 containing a 5-hydroxamate, amide, and reversed amide group, respectively, are also inactive. For 6-substituted 1-hydroxypyridin-2-one compounds, compounds 15 and 16 bearing a 6-phenyl and 6-(1-phenylethyl) group, respectively, are inactive against IDH1(R132H). Compound 17 with a 2-phenylethyl group exhibits less activity ($K_i = 10$ μM) compared with compound 7 with a 6-benzyl group. Compound 18, which has an additional $-CO_2Me$, is considerably less active than 17. These results, together with those of compounds 4–7, suggest that 6-benzyl is more favorable. In addition, despite the good activity of compound 8 with a 6-hydroxamic acid ($K_i = 4.5$ μM), we did not pursue this

Table 1. Structures and K_i Values of 5- or 6-Substituted Compounds against IDH1(R132H)


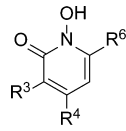
	R ⁵	R ⁶	K_i (μ M)
5	-Ph	-H	~50
4	-Bn	-H	8.2
10	-(CH ₂) ₂ Ph	-H	>50
11	-(CH ₂) ₃ Ph	-H	>50
6	-OPh	-H	46
12	-CONHOH	-H	>50
13	-CONHBn	-H	>50
14	-NHCOBn	-H	>50
15	-H	-Ph	>50
7	-H	-Bn	5.9
16	-H	-CH(CH ₃)Ph	>50
17	-H	-(CH ₂) ₂ Ph	10
18	-H	-(CH ₂) ₂ (4-CO ₂ Me-Ph)	27
8	-H	-CONHOH	4.5

compound further due to the high polarity as well as poor pharmacokinetics of the hydroxamate group.

Compound **2**, obtained by replacing the 6-cyclohexyl group of the inactive compound **9** with a benzyl substituent, was found to be a potent inhibitor of IDH1(R132H) with a K_i value of 190 nM, as shown in Table 2. It is ~30× more active than the analogous compound **7** without a 4-methyl group, showing the 4-Me is important for the activity. Compound **19** with 4-methyl-6-phenoxyethyl substituents was found to inhibit IDH1(R132H) with a K_i of 870 nM, ~4× less active than **2**. Compound **20** having 4,6-dimethyl substituents was found to be inactive. These results demonstrate that the combination of the 4-methyl and 6-benzyl substituents is needed to achieve a high inhibition.

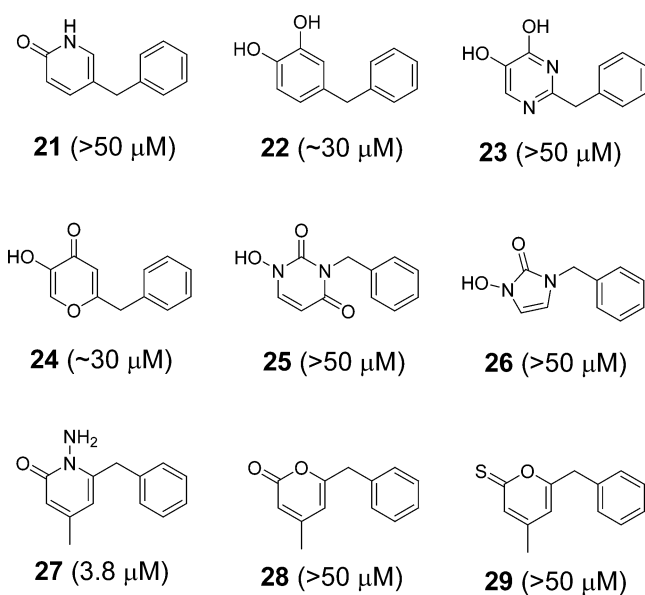
With the potent inhibitor **2** in hand, efforts were next made to optimize the 1-hydroxypyridin-2-one core structure. Chart 2 shows the structures and activities of compounds **21–29**, each of which has a different aromatic core structure, while contains a benzyl substituent for SAR analysis. Compared with compound **4**, lack of activity for compound **21** clearly indicates the importance of *N*-OH group. Greatly reduced activities for compounds **22–24** with a C-substituted -OH group suggest that the *N*-substituted -OH in compound **2** increases the binding affinity to IDH1(R132H). In addition, compared with compound **7** (Chart 1), lack of activity for compounds **25** and **26** suggests the reversely positioned *N*-OH and carbonyl functionalities are disfavored. Furthermore, compared with compound **2**, a 20-fold activity reduction for compound **27** ($K_i = 3.8 \mu$ M) with an *N*-NH₂ group again underscores the critical role of the *N*-OH group of the 1-hydroxypyridin-2-one core. Compounds **28** and **29** having a 2-pyrone and 2-thiopyrone ring, respectively, are also inactive. These SAR studies show that the 1-hydroxypyridin-2-one ring represents the most potent core structure for the inhibition of IDH1(R132H).

X-Ray Structure of Inhibitor Bound IDH1(R132H) and Structure Based Rationalization of SAR. We determined the X-ray structures of IDH1(R132H) in complex with NADPH and the potent inhibitors **2** and **3** at 3.3 Å,²¹ to a similar resolution as the previously reported structures.²⁵ Detailed structural information has been reported in our

Table 2. Structures and K_i Values of 3-, 4-, and 6-Substituted Compounds against IDH1(R132H)


	R ³	R ⁴	R ⁶	K_i (μ M)
9	-H	-Me	-cyclohexyl	>50
2	-H	-Me	-Bn	0.19
19	-H	-Me	-CH ₂ OPh	0.87
20	-H	-Me	-Me	>50
30	-Bn	-Me	-H	9.5
31	-CH ₂ (3-OMe-Ph)	-Me	-H	16.2
32	-CH ₂ (3-OH-Ph)	-Me	-H	13.6
33	-H	- <i>i</i> -Pr	-Bn	9.5
34	-H	-OH	-Bn	0.38
35	-H	-OMe	-Bn	5.5
36	-H	-CH ₂ OH	-Bn	5.6
37	-H	-CH ₂ OAc	-Bn	4.5
38	-H	-Me	-CH ₂ (4-OMe-Ph)	0.56
3	-H	-Me	-CH ₂ (4-OH-Ph)	0.28
39	-H	-Me	-CH ₂ (3-OMe-Ph)	0.15
40	-H	-Me	-CH ₂ (3-OH-Ph)	0.14
41	-H	-Me	-CH ₂ (2-OMe-Ph)	0.49
42	-H	-Me	-CH ₂ (2-OH-Ph)	0.65
43	-H	-Me	-CH ₂ (3-F-Ph)	2.2
44	-H	-Me	-CH ₂ (penta-F-Ph)	2.2
45	-H	-Me	-CH ₂ (4-CN-Ph)	12.5
46	-H	-Me	-CH ₂ (3-CN-Ph)	1.6
47	-H	-Me	-CH ₂ (3-COOH-Ph)	>50
48	-H	-Me	-CH ₂ (3-CONH ₂ -Ph)	8.5
49	-H	-Me	-CH ₂ (4-CF ₃ -Ph)	3.2
50	-H	-Me	-CH ₂ (3,5-diMe-Ph)	3.1
51	-H	-Me	-CH ₂ (thiophen-3-yl)	0.95
52	-H	-Me	-CH ₂ (3-biphenyl)	0.60
53	-H	-Me	-CH ₂ (4-OPh-Ph)	0.75
54	-H	-Me	-CH ₂ (naphth-1-yl)	0.95
55	-H	-Me	-CH ₂ (6-OMe-naphth-1-yl)	40.5
56	-H	-Me	-CH ₂ (6-OH-naphth-1-yl)	27.5
57	-H	-Me	-CH ₂ (benzothiophen-2-yl)	22.5
58	-H	-Me	-CH ₂ [4-(4-OMe-Ph)-Ph]	0.34
59	-H	-Me	-CH ₂ [4-(4-OH-Ph)-Ph]	0.25
60	-H	-Me	-CH ₂ [4-(3-OMe-Ph)-Ph]	0.14
61	-H	-Me	-CH ₂ [4-(3-OH-Ph)-Ph]	0.27
62	-H	-Me	-CH ₂ (3,5-diPh-Ph)	0.30

previous communication,²¹ while the interactions between the protein and **2** are briefly summarized to facilitate rationalization of SARs as well as inhibitor design described below. As shown in Figure 2a, the 4-methyl-1-hydroxypyridin-2-one ring of compound **2** is located in a pocket surrounded by Arg100, Ser94, Thr77, Asn96, Arg109, and NADPH. The planar -CONH₂ of Asn96 is located right underneath the pyridine ring of **2**, with the distance of ~4.1 Å. The two O atoms of the 1-hydroxypyridin-2-one core form two H-bonds with the two N atoms of the guanidinium group of Arg100. The calculated p*K*_a of 6.1 for **2** suggests that the *N*-OH group may be

Chart 2. Structures of 21–29 and Their K_i Values against IDH1(R132H)

deprotonated, which, together with the (partially negative) O atom of the 2-oxo group, also provides strong electrostatic interactions with the positively charged side chain of Arg100. This should explain why the core structures in compounds 21–24 and 27–29 with either a single O atom or a higher pK_a value are considerably less potent. The 4-methyl group is nicely fitted into a mainly hydrophobic cavity, ~3.7–4.2 Å from $-\text{CH}_3$ of Thr77 and $-\text{CH}_2-$ and $-\text{O}-$ of Ser94. Loss of these favorable interactions should account for the reduced activity of compound 7. The phenyl ring of the 6-benzyl has favorable hydrophobic (as well as electrostatic) interactions with the nicotinamide ring of NADPH, while the other side of the phenyl ring is ~5 Å away from the side chain of Arg109. In addition, the C4 atom of the phenyl ring is ~11 Å away from Leu250' (omitted in Figure 2a for clarity) from the other monomeric protein. Therefore, Arg109, Leu250', and NADPH form a relatively large pocket that could be explored for inhibitor design (described below). The crystal structures show compounds bearing a branched 6-substituent, such as 9, 15, and 16, would cause severe steric conflicts with NADPH if their 4-methyl-1-hydroxypyridin-2-one ring maintains the favorable interactions with the protein. This should account for the loss of activity for 9, 15, and 16.

Structure Guided Inhibitor Development and SAR. In the structure of the IDH1(R132H)/2 complex, there is a pocket near the 3-position of the 1-hydroxypyridin-2-one core, surrounded by Gly97, Lys93, Arg100, and Asn101. Compound 30, having a 3-benzyl as well as the favorable 4-methyl group, was designed and synthesized. Although it can be docked into the structure of IDH1(R132H)/2 with the binding pose of 1-hydroxypyridin-2-one core similar to that of 2 (Figure 2b), compound 30 exhibits a moderate inhibitory activity with a K_i of 9.5 μM (Table 2), being 50 \times less active than compound 2. Compounds 31 and 32 with additional meta-substituted -OMe and -OH are less active than 30. These results indicate that a benzyl group at the 3-position of the 1-hydroxypyridin-2-one ring is considerably less favorable than that at the 6-position.

We next sought to optimize the 4-position of the 1-hydroxypyridin-2-one ring. The IDH1(R132H)/2 structure

reveals that the 4-Me group has favorable interactions with the side chains of Thr77 and Ser94. Compared with 2, compound 33 with a 4-isopropyl group was found to exhibit a 50-fold activity loss ($K_i = 9.5 \mu\text{M}$), indicating that isopropyl is too bulky for the pocket. Compound 34 with a 4-hydroxyl group was found to be also a potent inhibitor of IDH1(R132H) with a K_i of 380 nM, being comparable to compound 2. Introducing the -OH was intended to have favorable interactions (e.g., H-bond) with the side chains of Thr77 (or Ser94), with the docking results of 34 shown in Figure 2c. However, the 4-OH in compound 34 is not superior to the 4-Me in 2. In addition, the 4-methoxy group in compound 35 ($K_i = 5.5 \mu\text{M}$) considerably reduces the inhibitory activity. Compound 36 with a 4-hydroxymethyl, as well as its acetyl ester 37, also have moderate potency with K_i values of 5.6 and 4.5 μM , respectively. These results show that only small substituents with a single heavy atom, such as -Me and -OH, are favorable for the 4-position of 1-hydroxypyridin-2-one ring. Because 1-hydroxypyridin-2-one compounds with a 4-methyl group is considerably easier to synthesize and might be more cell permeable than those with a 4-hydroxyl, we decided to keep the 4-Me for further SAR studies.

The SAR studies for the 6-position of compound 2 were performed to find a substituent that can provide increased potency. First, we wanted to explore how electron density of the phenyl ring affects the activity. Compound 38 with a *para*-OMe group in its 6-benzyl group exhibits less activity than does its parent compound 2, while 3 having a *para*-OH maintains a comparable activity ($K_i = 290 \text{ nM}$). Of interest are the higher inhibitory potencies of compounds 39 and 40 ($K_i = 150$ and 140 nM) having a *meta*-substituted OMe and OH group, respectively, showing that these two groups are more favorable. Changing the OMe and OH groups to the *ortho*-position for compounds 41 and 42 resulted in ~2 \times activity reductions with their K_i values of 490 and 650 nM, respectively. On the other hand, an electron-withdrawing fluoro substituent in 43 and 44 ($K_i = 2.2 \mu\text{M}$) was found to be highly disfavored, leading to ~10-fold activity decrease. A similar trend can be observed for compounds 45–49 (K_i 1.6 to >50 μM) bearing electron-withdrawing -CN, $-\text{CO}_2\text{H}$, $-\text{CONH}_2$, and $-\text{CF}_3$ groups, showing that strongly electron-deficient phenyl ring can reduce the inhibitory activity of this series of compounds. Compound 50 having two *meta*-substituted methyl groups possesses a moderate activity of 3.1 μM . Compound 51 bearing a thiophenyl side chain was found to be a good inhibitor ($K_i = 950 \text{ nM}$). The increased activity for compounds 39 and 40 might be due to increased interactions with Arg109, as show in Figure 2d for the docking results of 39. Introducing strong electron-withdrawing groups (e.g., -F, $-\text{CF}_3$, and -CN) for compounds 43–49 is disfavored because this could reduce the electrostatic interactions between the phenyl rings and the electron-deficient nicotinamide ring of NADPH.

Analogs with two or more aromatic rings at the 6-position of 1-hydroxypyridin-2-one were synthesized because of the relatively large pocket surrounded by NADPH, Arg109, and Leu250' described above. Compounds 52, 53, and 54 having a *meta*-biphenyl, *para*-phenoxyphenyl, and 1-naphthyl group, respectively, were found to be strong inhibitors with K_i values of 600, 750, and 950 nM. However, compounds 55 and 56, which are derivatives of 54 with a 6-OMe or -OH in the naphthyl ring, respectively, exhibit very weak activity ($K_i > 25 \mu\text{M}$). Similarly weak activity was observed for the benzothio-phenyl derivative 57 ($K_i = 22.5 \mu\text{M}$). These three compounds

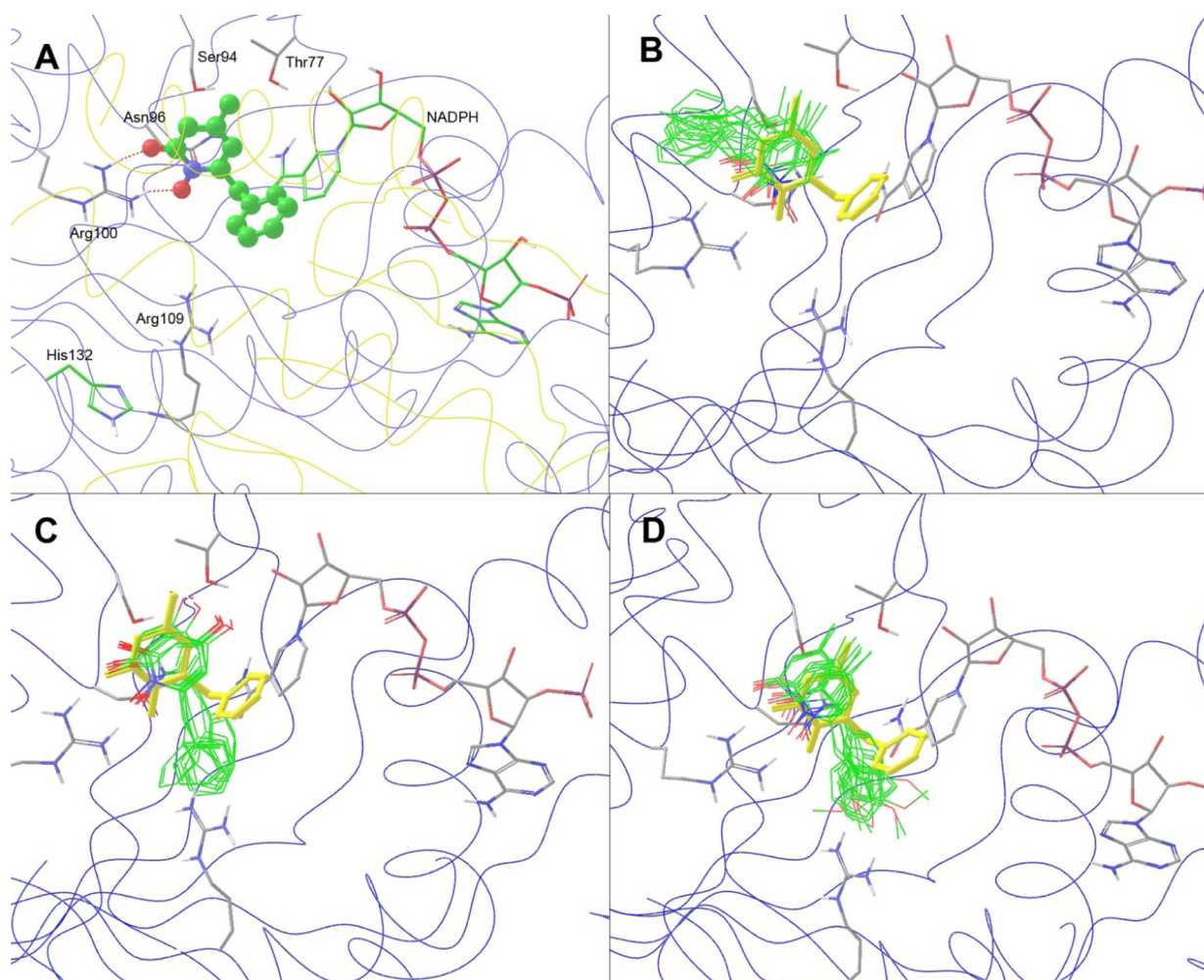


Figure 2. X-ray crystal and docking structures of inhibitors of IDH1(R132H). (A) The close-up view of the active site of the crystal structure of IDH1(R132H)/2, with the backbone of one monomeric protein shown in blue lines and that of the other monomer in yellow. Compound 2 is shown as a ball and stick model. Only selected residues with the interactions with 2 are shown for clarity. (B) Ten docking structures of compound 30 (with C atoms in green), superimposed with the crystal structure of 2 (in yellow), showing that the 3-benzyl group of 30 is predicted to occupy an empty pocket. (C) Ten docking structures of compound 34 (with C atoms in green), superimposed with the crystal structure of 2 (in yellow), showing the 4-OH group of 34 is predicted to have favorable interactions with Thr77. (D) Ten docking structures of compound 39 (with C atoms in green), superimposed with the crystal structure of 2 (in yellow), showing the 6-(3-OMe-Ph) group of 39 is predicted to have favorable interactions with Arg109.

are >23× less active than their parent compounds 54 and 51. Compounds 58 and 59 with a *para*-OMe and *para*-OH substituted *para*-biphenyl group were, however, found to be potent inhibitors of IDH1(R132H) with K_i values of 340 and 250 nM, respectively. Moving the OMe and OH groups to the *meta*-position for compounds 60 and 61 resulted in more potent inhibition, with the K_i values of these two compounds being 140 and 270 nM, respectively. Finally, compound 62 bearing a *meta*-terphenyl group was found to be still a potent inhibitor ($K_i = 300$ nM). Activity data of these compounds show a large variety of substituents with different sizes can replace the phenyl moiety of compound 2 while maintaining comparable or having even improved activity. More modifications at this position could further improve the inhibitory activity.

Inhibition of IDH1(R132C) and WT IDH1. Although rare in glioma, Arg132 mutation to cysteine in IDH1 is frequently found in acute myeloid leukemia and sarcomas.^{6,9–11} The mutant protein IDH1(R132C) possesses the same enzymatic function as IDH1(R132H) (Figure 1C) with comparable

kinetic parameters.⁶ The R132C mutation also causes elevated levels of D2HG in these cancer patients.

We selected 10 representative IDH1(R132H) inhibitors, with K_i values ranging from 0.14 to 9.5 μ M, and tested the activity of these compounds against recombinant IDH1-(R132C), using our previous method.²¹ The results, together with their K_i values against IDH1(R132H), are summarized in Table 3. These compounds were found to also be inhibitors of IDH1(R132C) with K_i values ranging from 0.12 to 14.7 μ M, which shows a good correlation with those for the R132H mutant enzyme, with R^2 of 0.83 as well as slope of 1.04 (Figure 3A). These results suggest that the residue Cys132 seems to have a similar function as His132 does for catalyzing the reduction of α -KG to D2HG.

Next, given that WT IDH1 plays an important role in normal physiology, an ideal inhibitor should have a good selectivity for the mutant IDH1 enzymes. The inhibitory activities of the above 10 compounds were tested against recombinant WT IDH1 and the results are also shown in Table 3. Compounds 2, 3, and 58–60 were found to have only weak inhibitory

Table 3. Activity of Selected Inhibitors of Mutant IDH1

	IDH enzyme K_i (μM)			IC_{50} (μM) for inhibition of D2HG
	WT	R132H	R132C	
2	12.3 \pm 3.1	0.19 \pm 0.04	0.12 \pm 0.03	2.4 \pm 0.5
3	16.8 \pm 3.0	0.28 \pm 0.07	0.27 \pm 0.07	8.5 \pm 2.5
4	>50	8.2 \pm 2.1	6.6 \pm 2.6	<i>a</i>
7	>50	5.9 \pm 1.3	10.5 \pm 3.2	>30
8	>50	4.5 \pm 1.7	2.4 \pm 0.4	<i>a</i>
33	>50	9.5 \pm 2.9	14.7 \pm 6.3	>30
34	>30	0.38 \pm 0.08	1.8 \pm 0.5	9.7 \pm 1.8
39	>30	0.15 \pm 0.05	0.26 \pm 0.07	1.1 \pm 0.2
40	>30	0.14 \pm 0.07	0.42 \pm 0.11	3.8 \pm 0.8
58	14.0 \pm 2.9	0.34 \pm 0.08	0.80 \pm 0.31	1.1 \pm 0.3
59	15.2 \pm 5.1	0.25 \pm 0.1	0.56 \pm 0.24	3.2 \pm 0.3
60	13.0 \pm 3.5	0.14 \pm 0.04	0.62 \pm 0.21	6.3 \pm 0.8

^aNot tested.

activities (K_i 12.3–16.8 μM) against WT IDH1, while compounds 7, 33, 34, 39, and 40 do not inhibit the enzyme. Selectivity of >41-fold was observed for these compounds, compared with their K_i values against IDH1(R132H).

The activities of these compounds against the three IDH1 enzymes indicate that Arg132 exhibits a drastically different role from His132 or Cys132. Previous structural studies of WT and R132H mutant IDH1 show IDH1(R132H) has two ligand binding sites, I and II (Supporting Information Figure S1A),²⁵ with the site II being the catalytic site \sim 6.5 Å away from site I, while WT IDH1 only has the binding site II. ICT binds to site I in IDH1(R132H), while α -KG occupies the catalytically active, binding site II.^{12,25} His132 is not involved in the binding of either ICT or α -KG. ICT is located in site II in WT IDH1. The function of Arg132 is to have two H-bonds as well as an electrostatic interaction with the two carboxyl groups of ICT, which can enhance the binding of ICT in site II as well as stabilize the overall structure of the IDH1/ICT complex. Due to the shorter length as well as the chemical nature of the side chain, His132 (as well as Cys132) cannot play the same role as Arg132. This explains why R132H and R132C mutant proteins have the similar function, while WT IDH1 having Arg132 is a different enzyme. It is noted that the two binding sites I and II do not coexist in IDH1(R132H). With ligand induced protein conformational changes, IDH1(R132H) exhibits either its binding site I or II.

Our X-ray crystallographic studies showed that compounds 2 and 3 are located in the ligand binding site I of IDH1(R132H) (Supporting Information Figure S1B,C).²¹ The R132H (as well as R132C) mutation causes the mutant protein to bind ICT/2/

3 in the binding site I, while R132 in WT IDH1 can induce protein conformational changes and stabilize the binding of ICT/ α -KG in the site II. Our modeling studies show that the distinct environment for binding site I represents the structural basis for the high selectivity of inhibitors 2 and 3 for mutant IDH1.²¹

Inhibition of Cellular Production of D2HG. The hallmark of IDH mutated cancer is the significantly elevated D2HG concentrations in cancer cells as well as in plasma. We next measured the ability of the 10 inhibitors in Table 3 to reduce the cellular production of D2HG. Human fibrosarcoma HT1080 cells, which harbor the IDH1 R132C mutation,²⁶ were treated with increasing concentrations of these compounds for 48 h. No significant cytotoxicity to HT1080 cells was observed for up to 30 μM . D2HG concentrations of the cells were quantitatively determined by using HPLC-MS. Are shown in Table 3, except for the weak inhibitors 7 and 33 (used as negative controls), inhibitors of IDH1(R132C) were able to inhibit the production of D2HG in HT1080 with the IC_{50} values of 1.1–9.7 μM . In addition, the cell activities of these compounds also exhibit a good correlation with their enzyme activity, showing a R^2 value of 0.73 (Figure 3B).

In vitro Blood–Brain Barrier (BBB) Permeability. Since inhibitors of mutant IDH1 are required to penetrate the blood–brain barrier (BBB) for glioma treatment, a cell-based model system using MDCK-MDR1 cells^{27,28} was used to determine the BBB permeability potential for selected compounds 2 and 39, as well as for the known inhibitor 1 as a comparison. The cells are grown on polycarbonate supports separating two chambers to allow compound flux in either direction, apical [A] to basolateral [B] and vice versa, to be measured. The cells are highly confluent to approximate the tight junctions characteristic of endothelial cells that comprise the BBB. In addition, the multidrug resistance 1 (*MDR1*) gene is overexpressed in the cell, producing a high level of P-glycoprotein (the product of *MDR1*), a known BBB efflux pump, on the apical side that limits brain distribution for many low molecular weight drugs.

As can be seen in Table 4, 1-hydroxy-pyridin-2-one compounds 2 and 39 were both found to have analogous cell

Table 4. Cell Permeability Rates (10^{-6} cm/s) for Mutant IDH1 Inhibitors

	rate (apical to basolateral)	rate (basolateral to apical)	efflux ratio ^a
1	0.15	10.4	72.6
2	5.45	6.34	1.3
39	5.39	8.88	1.7

^aMeasured as $\text{rate}^{(B \rightarrow A)} / \text{rate}^{(A \rightarrow B)}$.

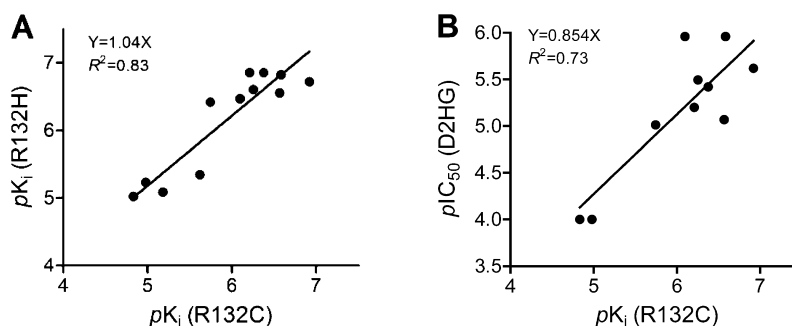


Figure 3. Correlations between inhibition of IDH1(R132C) and that of (A) IDH1(R132H) and (B) cellular production of D2HG.

permeability values of 5.45 and 5.39, respectively, in the A → B direction, and possessed comparable rates of 6.34 and 8.88 for the reverse direction. The low efflux ratios (1.3 and 1.7) due to the comparable directional permeability rates suggest that these two compounds are not likely substrates for P-glycoprotein. On the other hand, compound **1** exhibited a low rate of cell permeability (0.15) in the A → B direction and much higher rate of 10.4 in the B → A direction leading to a high efflux ratio of 72.6, suggesting that compound **1** is a substrate of P-glycoprotein and likely BBB impermeable.

Selective Activity against Glioma Stem-Like Cells with IDH1 R132H Mutation. Next, we examined the activity of the IDH1(R132H) inhibitors against BT-142 glioma cells having the R132H IDH1 mutation,²⁹ as well as two glioma cells, BXD-4687 and -3752, without an IDH1 mutation as controls.^{30,31} Unlike normal cell culture conditions under which cells are grown as a monolayer attached to a plate, these glioma cells were cultured in serum-free media and grown as neurospheres, colonies of glioma cells with a diameter of 30–300 μm. The so-called cancer stem cells (CSC) are enriched in these neurospheres.^{32–34} CSCs represent a small fraction of cancer cells with a distinct phenotype that can form new tumors when transplanted into immunocompromised mice.^{30,35–37} While proliferating rapidly, the bulk non-stem cancer cells fail to do so. CSCs possess certain key traits as normal stem cells, including the ability to unlimitedly self-renew and differentiate. It has now well documented that CSCs play important roles in antitumor-drug resistance, cancer relapse, and metastasis. It is therefore important to find compounds having selective activity against CSCs.

The most potent IDH1(R132H) inhibitors **2**, **39**, **40**, **58**, and **59** were tested to inhibit the formation of neurospheres of the three glioma cells. Also included in the assay are compound **1** and temozolomide, the first-line chemotherapy for glioblastoma. As shown in Table 5, all of the three clinical glioblastoma

Table 5. EC₅₀ Values (μM) of Selected Inhibitors against Glioma and Normal Fibroblast WI-38 Cells

	BT-142	BXD-4687	BXD-3752	WI-38
temozolomide	>50	>50	>50	^b
1	>20 ^a	>20	>20	>50
2	0.37 ± 0.2	6.8 ± 1.2	5.9 ± 1.1	>50
39	0.63 ± 0.2	1.2 ± 1.3	2.5 ± 1.3	>50
40	1.8 ± 0.6	7.5 ± 3.1	6.2 ± 1.2	>50
58	0.26 ± 0.2	7.6 ± 1.4	2.8 ± 1.3	>50
59	0.69 ± 0.4	16 ± 2.0	5.1 ± 1.1	>50

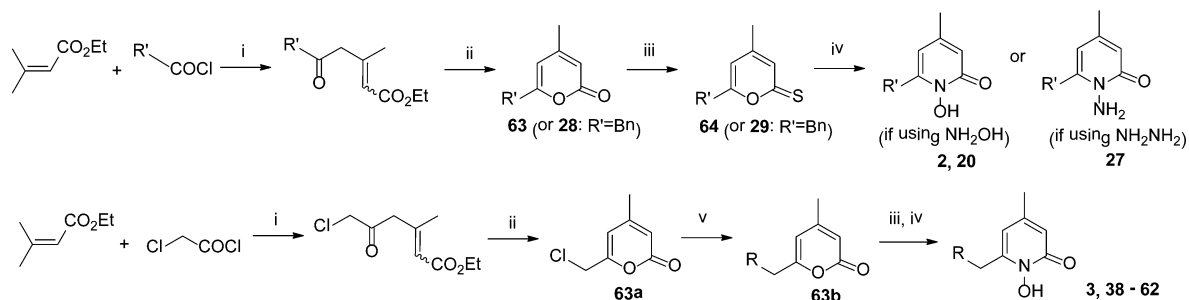
^aEC₅₀ of **1** cannot be accurately determined; **1** (2 μM) exhibited ~40% of inhibition, but increasing to 20 μM still showed ~40% inhibition. ^bNot tested.

cells are resistant to temozolomide (EC₅₀ > 50 μM), suggesting that these cells overexpress *MDR1*, which is the main cause for temozolomide resistance. Compound **1** exhibits no activity against BXD-4687 and -3752 (without an IDH1 mutation) and normal fibroblast WI-38 cells. For BT-142 glioma cells with the IDH1 R132H mutation, **1** was found to inhibit neurosphere formation by ~40% at 2 μM, but increase of the concentration of **1** to 20 μM did not result in higher inhibition, presumably due to the high efflux or poor permeability of **1** (Table 4). Consistent with the results in Table 4, activity of compound **2** (as well as other 1-hydroxypyridin-2-one analogs) is not affected by these factors. Compound **2** exhibited potent activity

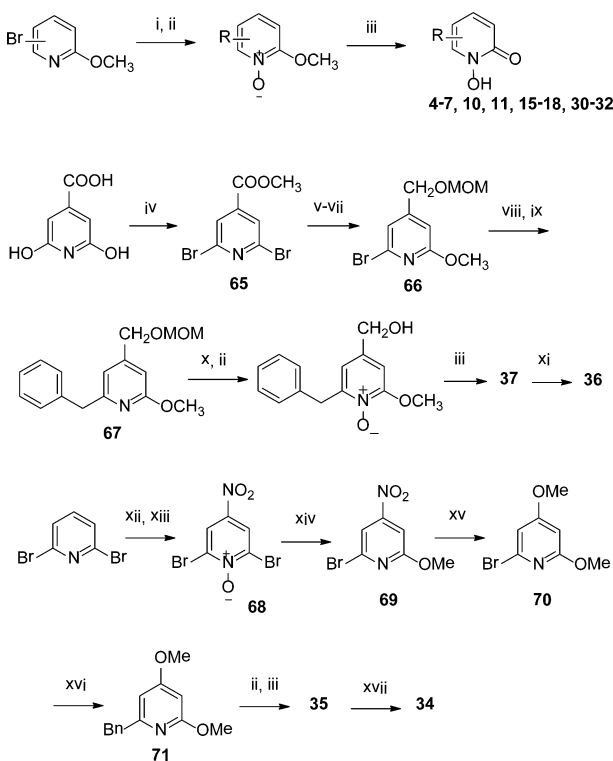
against IDH1(R132H)-containing BT-142 cells with an EC₅₀ of 370 nM, while it had significantly weaker activity against BXD-4687 and -3752 without an IDH1 mutation (EC₅₀ 6.8 and 5.9 μM, respectively), showing a high selectivity of ~16-fold. In addition, compound **2** possesses negligible cytotoxicity against the proliferation of normal fibroblast WI-38 cells (EC₅₀ > 50 μM, Table 4). These results show that potent IDH1(R132H) inhibitor **2** possesses selective activity against the proliferation of CSCs of BT-142, which is dependent upon the cellular environment caused by a high concentration of D2HG. The moderate activity of **2** against BXD-4687 and -3752 suggests the compound could have nonspecific activity against the proliferation of these two glioma cells. Indeed, while inactive against IDH1(R132H), compound **9** (ciclopirox) was reported to have similar (low micromolar) antiproliferative activity against, for example, breast cancer and leukemia cells.^{38,39} This suggests compound **2** exerts dual activities on BT-142 cells, that is, by inhibiting IDH1(R132H) and blocking rapid proliferation simultaneously, which could provide a synergistic (or additive) effect. This could explain the high potency of the dual-role compound. Similarly, compounds **39**, **40**, **58**, and **59** exhibited selective activity against BT-142 glioma cells, with compound **58** being the most potent. It inhibited neurosphere formation of BT-142 with an EC₅₀ of 260 nM, while it showed >10-fold less activity against the two glioma cells without an IDH1 mutation. Moreover, none of these compounds possess significant cytotoxicity against the proliferation of normal fibroblast WI-38 cells, showing potentially low toxicity. Given temozolomide resistance in a significant portion of glioma/glioblastoma as well as poor BBB permeability and weak antiglioma activity of compound **1**, these results demonstrate the importance for further development of these 1-hydroxypyridin-2-one inhibitors as potential therapeutics for IDH1 mutated glioma.

Chemistry. Scheme 1 shows the general methods for the synthesis of the 4-methyl-6-substituted 1-hydroxypyridin-2-one and related compounds, which include the most active inhibitors (e.g., **2** and **39**) of mutant IDH1. An acyl chloride was reacted with ethyl 3-methyl-2-butenate in the presence of AlCl₃ to produce a mixture of stereoisomeric esters, which without purification were cyclized under acidic conditions to generate a single compound, pyron-2-one **63**, with a yield of 50–85% from the acyl chloride. Because the reaction of **63** with hydroxylamine occurred in a very poor yield (0–20%), compound **63** was converted to more reactive pyron-2-thione **64**,⁴⁰ which reacted readily with hydroxylamine or hydrazine to give 4-methyl-6-substituted 1-hydroxy (or amino)-pyridin-2-one compounds in 67–73% yield. We found that compound **63a** with a 6-chloromethyl group is a useful common intermediate, which can undergo a mild Suzuki coupling reaction to give **63b**. With this route, compounds **3** and **38–62** were synthesized without each starting from a different acyl chloride. In addition, strong acid sensitive R-groups, for example, thiophenyl in **51**, can be introduced.

The majority of the mono-5- or 6-substituted 1-hydroxypyridin-2-one compounds were synthesized using a palladium catalyzed coupling reaction starting from a bromo-substituted 2-methoxypyridine (Scheme 2). By our previous methods,²¹ the 2-methoxypyridine moiety of the coupling products was converted to the 1-hydroxypyridin-2-one core by oxidation with 3-chloroperoxybenzoic acid followed by treatment with acetyl chloride. To synthesize compounds **36** and **37**, 2,6-dihydroxyisonicotinic acid was heated with POBr₃ followed by

Scheme 1. Synthesis for 4-Methyl-6-substituted 1-Hydroxypyridin-2-one and Related Compounds^a

^aReagents and conditions: (i) AlCl_3 , CH_2Cl_2 , reflux; (ii) $\text{H}_2\text{SO}_4/\text{HOAc}$; (iii) P_4S_{10} , benzene, reflux; (iv) NH_2OH or NH_2NH_2 , pyridine, reflux; (v) R-B(OH)_2 , $\text{Pd(dppf)}\text{Cl}_2$, dioxane, reflux.

Scheme 2. Synthesis for Other Compounds^a

^aReagents and conditions: (i) a Pd-catalyzed coupling reaction, for example, Suzuki or Heck reaction; (ii) 3-chloroperoxybenzoic acid; (iii) AcCl , reflux, then MeOH ; (iv) POBr_3 , 130°C , then MeOH ; (v) NaBH_4 , reflux; (vi) MOMCl , Et_3N ; (vii) NaOMe , reflux; (viii) BuLi , -78°C , then PhCHO , 25°C ; (ix) Et_3SiH , trifluoroacetic acid, 50°C ; (x) 3 N HCl ; (xi) NaOH ; (xii) H_2O_2 , TFA , reflux; (xiii) HNO_3 , H_2SO_4 , 60°C ; (xiv) PBr_3 ; (xv) NaOMe , MeOH/THF , 40°C ; (xvi) BnZnBr , $\text{Pd(PPh}_3)_4$, THF , reflux; (xvii) BBr_3 , CH_2Cl_2 .

methanolysis to give 2,6-dibromo ester **65**, which was reduced, protected with a methoxymethyl (MOM) group, and treated with NaOMe to produce compound **66** with the desired 2-OMe and 6-Br. Treatment with BuLi followed by benzaldehyde afforded a secondary alcohol, whose $-\text{OH}$ was reduced by the reaction with Et_3SiH and trifluoroacetic acid⁴¹ to give compound **67**. Deprotection of MOM as well as conversion to 1-hydroxypyridin-2-one led to the formation of compound **37**. Hydrolysis of **37** with NaOH produced compound **36**. Compounds **34** and **35** were prepared from 2,6-dibromopyridin-4(1H)-one (Scheme 2). The oxidation of the pyridine ring facilitated

the nitration at the 4-position of 2,6-dibromopyridin-4(1H)-one to give compound **68**. Upon reduction of the pyridine-oxide, treatment with NaOMe resulted in double substitutions of the 2-Br and 4- NO_2 groups to give 6-bromo-2,4-dimethoxypyridin-4(1H)-one (**70**). A palladium catalyzed reaction to introduce the 6-benzyl group followed by conversion to 1-hydroxypyridin-2-one gave rise to compound **35**, whose $-\text{Me}$ was removed by treatment with BBr_3 to produce compound **34**.

CONCLUSION

IDH1 mutations at the residue Arg132 are frequently found in low grade gliomas/secondary glioblastomas (~75%), AML (~20%), and certain sarcomas. Studies have shown that these mutant proteins acquire a new enzyme function, that is, the reduction of $\alpha\text{-KG}$ to D2HG, causing D2HG accumulation in the patients. High concentrations (in millimolar levels) of D2HG can inhibit a broad range of $\alpha\text{-KG}$ -dependent dioxygenases, including histone demethylases and DNA hydroxylases, leading to abnormal levels of histone/DNA methylation, which block cell differentiation and eventually cause cancer initiation. Mutant IDH1 proteins are therefore drug targets for these types of cancer. Upon screening of compounds targeting another $\text{Mg}^{2+}/\text{NADPH}$ -dependent enzyme, 1-hydroxypyridin-2-one compounds **4** and **7** were identified to be low micromolar inhibitors of IDH1(R132H). Guided by SAR as well as the X-ray structure of the IDH1(R132H)/**2** complex, a total of 61 derivatives were designed and synthesized, among which several potent inhibitors were identified with K_i values of 140–270 nM. SAR analysis shows that (1) the 1-hydroxypyridin-2-one core structure is required to be active, (2) a very small group such as $-\text{Me}$ or $-\text{OH}$ at the 4-position of the core is needed to achieve a submicromolar potency, (3) a (substituted) benzyl group at the 6-position of 1-hydroxypyridin-2-one is more favored compared with a phenyl or other groups at the 3- and 5-positions, and (4) strongly electron-withdrawing groups are disfavored as a substituent for the 6-benzyl, while $-\text{OMe}$ or $-\text{OH}$, for example, that in compounds **39**, **40**, and **60**, provides an improved activity. Ten selected compounds were tested for their activity in inhibiting IDH1(R132C), as well as the production of D2HG in HT1080 fibrosarcoma cells, and the results indicate that there are good correlations between these inhibitory activities. In addition, these compounds exhibit potent and selective activity in inhibiting the proliferation of BT-142 glioma cells with the R132H IDH1 mutation, with the most potent compound **58** having EC_{50} of $0.26\ \mu\text{M}$, while it is considerably less active against two glioma cells without an

IDH1 mutation (EC_{50} 2.8 and 7.6 μ M), showing a selectivity of >10-fold. Low cytotoxicity (EC_{50} > 50 μ M) of these compounds against normal fibroblast WI-38 cells was observed. Moreover, using a cell based BBB model assay, 1-hydroxypyridin-2-one inhibitors were found to be BBB permeable, while inhibitor **1** with another chemo-type has a high efflux ratio, which might be responsible for the observed weak activity of **1** (EC_{50} > 20 μ M) against BT-142 glioma cells. All these results suggest that this work could lead to a new treatment for IDH1 mutated glioma and further development of 1-hydroxypyridin-2-one inhibitors is warranted.

EXPERIMENTAL SECTION

All reagents were purchased from Alfa Aesar (Ward Hill, MA) or Aldrich (Milwaukee, WI). Compounds were characterized by 1 H NMR on a Varian (Palo Alto, CA) 400-MR spectrometer, and the purities monitored by a Shimadzu Prominence HPLC with a Phenomenex C18 column (4.6 mm \times 250 mm, methanol/H₂O 60:40, monitored at 254 and 280 nm). The purities of all compounds were found to be >95%.

Synthesis and Characterization of Compounds 2–62. Details of compound synthesis and characterization can be found in Supporting Information, Experimental Section.

Expression and Purification of Human WT and R132H Mutant IDH1. The wild-type IDH1 gene was cloned using 5'-GATCCGAATTCGATGTCCAAAAAATCAGTG-3' and 5'-TGG-TGCTCGAGTAAGTTTGGCCTGAGCTAG-3' as forward and reverse primers, respectively, and inserted into pET-24b vector. Correctness of the inset was verified by sequencing. *Escherichia coli* BL21-CodonPlus strain (Agilent) was transformed with the plasmid and cultured at 37 °C in LB medium containing kanamycin (50 μ g/mL) and chloramphenicol (34 μ g/mL). Upon reaching an optical density of \sim 0.6 at 600 nm, IDH1 expression was induced by addition of 0.1 mM isopropylthiogalactoside at 18 °C for 20 h. Cells were harvested, lysed, and centrifuged at 20000 rpm for 20 min, and the supernatant was collected and purified using Ni-affinity (HisTrap HP, GE Healthcare) followed by Superdex 75 (GE Healthcare) column chromatography. WT-IDH1 was obtained with \sim 90% purity (SDS-PAGE).

R132H and R132C mutant IDH1 genes were generated from the wild-type IDH1 plasmid, using QuikChange site-directed mutagenesis kit (Agilent) following the manufacturer's protocol. Correctness of the gene sequences was verified. The mutant genes were then transferred to pGEX-KG vector for better expression. Expression of mutant IDH1 enzymes were performed similarly to that for the wild-type protein. Cells were harvested, lysed, and centrifuged at 20000 rpm for 20 min, the supernatant was collected, and the recombinant protein was trapped in glutathione sepharose resin (GE Healthcare). The GST-IDH1 fusion protein was eluted with 10 mM glutathione solution, and the GST tag was removed by thrombin digestion overnight at 4 °C. IDH1(R132H) and IDH1(R132C) were obtained in \sim 90% purity (SDS-PAGE) using a glutathione sepharose column followed by Superdex 75 gel filtration column chromatography.

Enzyme Inhibition Assays. Determination of the activity and inhibition of IDH1(R132H) and IDH1(R132C) is based on the initial linear consumption of NADPH in the reaction. The enzyme activity assay was performed in a 96-well microplate using the purified IDH1 mutant (100 nM), 4 mM MgCl₂, 1 mM α -KG, and 100 μ M NADPH ($\gg K_m$ for NADPH) in 50 mM 4-(2-hydroxyethyl)-1-piperazineethanesulfonic acid (HEPES) buffer (pH = 7.5) containing 0.1 mg/mL bovine serum albumin. For inhibition assays, triplicate samples of compounds were incubated with the protein for 5 min before addition of α -KG to initiate the reaction. The optical absorbance of each well was monitored every 30 s at 340 nm, where NADPH has maximum absorption, using a Beckman DTX-880 microplate reader. The data were imported into Prism (version 5.0, GraphPad), and the IC_{50} values were calculated with a standard dose–response curve fitting. For compounds with IC_{50} values much greater than the enzyme

concentration, K_i values were calculated using the Cheng–Prusoff equation $K_i = IC_{50}/(1 + [S]/K_m)$, where [S] is the concentration of α -KG (1 mM) and K_m is the literature value of 0.965 mM for R132H¹² and 0.295 mM for R132C.⁶ For compounds with IC_{50} < 1 μ M, K_i values were calculated using the Morrison tight inhibition modeling in Prism.

Determination of the activity/inhibition of WT-IDH1 is based on the initial linear production of NADPH. In brief, the enzyme activity assay was performed in a 96-well microplate using the purified IDH1 (15 nM), 4 mM MgCl₂, 200 μ M sodium D-isocitrate ($K_m = 65 \mu$ M),¹² and 1 mM NADP⁺ ($\gg K_m$ for NADP) in 50 mM HEPES buffer (pH = 7.5). The reaction can be readily monitored by an increase in optical absorbance at 340 nm. Activity and compound inhibition can be determined similarly as described for mutant IDH1 using Prism 5.0.

Docking. Docking studies were performed with our previous methods^{21–23} using the Schrödinger suite (version 2013, Schrödinger, LLC, New York, NY, 2013), which includes all of the programs described below. The crystal structure of IDH1(R132H)/2 (PDB 4I3L) was prepared using the module “protein preparation wizard” in Maestro (version 9.5) using default protein parameters, with all water molecules removed, hydrogens added, inhibitor extracted, and NADPH retained in the protein structure for docking. H-bonds were then optimized, and the protein was energy-minimized using OPLS-2005 force field. A receptor grid, which is large enough to contain the whole active site, was generated using Glide (version 5.5) without constraints. Compounds were built, minimized using OPLS-2005 force field in Maestro, and then docked into the prepared protein structure using Glide (docking parameters: standard-precision and dock flexibly).

Cell Growth Inhibition. The cytotoxicity assay was done using our previous method.^{21,22} In brief, 10⁵ WI-38 fibroblast cells were inoculated into each well of a 96-well plate and cultured in Dulbecco's modified Eagle's medium (DMEM) supplemented with 10% fetal bovine serum at 37 °C in a 5% CO₂ atmosphere with 100% humidity overnight for cell attachment. After addition of compounds (from 1 to 50 μ M), plates were incubated for 48 h, after which cell viability was assessed by the 3-(4,5-dimethylthiazol-2-yl)-2,5-diphenyltetrazolium bromide (MTT) assay, using a commercially available kit (Sigma). IC_{50} value of each compound was calculated from dose–response curves by Prism 5.0.

D2HG Production Inhibition in HT1080 Cells. The HT1080 fibrosarcoma cell line, which harbors an IDH1(R132C) mutation, was obtained from ATCC (Manassas, VA). The D2HG production inhibition assay followed our previous protocol.²¹ In brief, 10⁵ cells/well were seeded into wells of a six-well plate and cultured in Dulbecco's modified Eagle's medium (DMEM) supplemented with 10% dialyzed fetal bovine serum at 37 °C in a 5% CO₂ atmosphere with 100% humidity overnight for cell attachment. Cells were treated with an increasing concentration of compounds in 2 mL of culture medium for 48 h. Medium was collected and diluted with 8 mL of MeOH. After shaking, the mixture was centrifuged to remove any precipitate, and the supernatant was subjected to HPLC-MS to separate and quantitate the amount of D2HG. HPLC was run using a Phenomenex C18 column (250 mm \times 4.6 mm, 5 μ m) with 50% tributylamine buffer/50% MeOH as an eluent at a flow rate of 0.5 mL/min (tributylamine buffer: 10 mM tributylamine, 15 mM acetic acid, 3% MeOH in water). A single ion monitoring (SIM) for 147 Da was used to detect and quantitate the amount of D2HG (parameters: interface voltage, -4.2 kV; detector voltage, 1.3 kV; nebulizing gas, 1.5 L/min; drying gas, 15 L/min; desolvation line temperature, 250 °C; heat block temperature, 200 °C; Pirani gauge vacuum, 102 Pa; ion gauge vacuum: 5×10^{-4} Pa). Authentic D2HG purchased from Sigma-Aldrich (St Louis, MO) was used to validate and calibrate the HPLC-MS assay conditions before measuring the D2HG concentrations secreted by the HT1080 cells untreated or treated with **2**. EC_{50} was calculated from the dose–response curve by Prism 5.0.

In Vitro Blood–Brain Barrier (BBB) Permeability Assay. MDCK-MDR1 cells were obtained from NIH (Bethesda, MD) and maintained in DMEM with 10% standard fetal bovine serum, 100 U/mL penicillin, 100 μ g/mL streptomycin, and 80 ng/mL colchicine. For

transport experiments, cells with passage numbers of 24–33 were seeded at a density of 60000 cells/cm² on Transwell plates (pore size 0.4 μm; diameter 6.5 mm; insert growth area 0.33 cm²; Costar, Pittston, PA) and maintained in culture as previously described.²⁸ In brief, confluent MDCK-MDR1 monolayers expressing P-glycoprotein were obtained 3–4 days postseeding, and their integrity was assessed by measurement of the transepithelial electrical resistance (TEER, Ω·cm²) with a volt–ohm meter (Millicell-ERS, Millipore Corporation, Billerica, MA). After subtraction of the background TEER (i.e., the resistance exhibited by the filter alone), only MDCK-MDR1 cell monolayers that exhibited a TEER > 1000 Ω·cm² throughout [measured before and after the study] the experiments were used.

Drug transport across the cell monolayers was measured in both apical to basolateral (A-B) and basolateral to apical (B-A) directions. Experiments were performed in HBSS (Hank's balanced salt solution containing 50 mM HEPES buffer, pH ≈ 7.4) at 37 °C using monolayers that were preincubated for 30 min with prewarmed HBSS. At the start of the experiment, fresh HBSS was added to the receiver compartments, and the compounds were independently added to the donor compartments at an initial concentration of 10 μM (diluted from 10 mM DMSO stock to a final DMSO concentration of 0.1%) and then incubated at 37 °C for 90 min, after which samples were collected from both the receiver and donor compartments.

Detection and quantification of the compounds were performed with an LC/MS/MS system (HPLC, Shimadzu, Kyoto, Japan; MS, QTrap 5500, Applied Biosystems, Foster City, California) using an electrospray ionization (ESI) interface and operated in positive ion mode. Instrument control, data acquisition, and processing for both chromatography and MS were performed using the Analyst 1.5.1 software (Applied Biosystems MDS Sciex, Ontario, Canada). The chromatographic separation system consisted of a guard cartridge (C18, 4.0 × 2.0 mm²; Phenomenex, Torrance, California), an analytic column (Luna C18, 3 μm particle size, 50 × 2.0 mm²; Phenomenex), and a mobile phase of acetonitrile/10 mM ammonium formate (65:35, v/v), delivered isocratically at a flow rate of 0.2 mL/min. To 10 μL samples from both the apical or basolateral sides, 40 μL of cold acetonitrile was added; samples were mixed and centrifuged at 15000 rpm for 5 min; 10 μL of the resultant supernatant was injected into the LC/MS-MS system. Compound quantification was performed by ESI-selected reaction monitoring. The column effluent was monitored at the following precursor–product ion transitions: *m/z* 214.9 → 197.1 for compound 2, *m/z* 244.9 → 212.3 for 39, and *m/z* 463.2 → 123.0 for 1 with a dwell time of 100 ms for each ion transition.

The apparent permeability, P_{app} (cm/s) was calculated as $P_{app} = dQ / (dt \times 1 / (AC_0))$, where dQ/dt is the transport rate of the compound (mol/s), A is the area of the cell monolayer (cm²), and C_0 is the initial donor concentration (mol/L).

Inhibition of the Proliferation of Glioma Cells. Two glioma neurosphere cultures, Baylor xenograft derived BXD-4687 and BXD-3752, were initiated from patient tumor-derived orthotopic xenograft mouse models.^{30,31} These cells were cultured in serum-free cell growth medium consisting of neurobasal media, N2 and B27 supplements (Life Technologies, Grand Island, NY), recombinant human bFGF and EGF (50 ng/mL each; R&D Systems Inc., Minneapolis, MN), 200 units/mL penicillin, and 200 μg/mL streptomycin at 37 °C in a 5% CO₂ atmosphere with 100% humidity as we described previously.^{30,31} BT-142 glioma cells,²⁹ which have an endogenous R132H mutation in IDH1, aggressive tumor-initiating capacity, and 2-hydroxyglutarate (2-HG) production, were obtained from ATCC (Manassas, VA) and maintained in above-mentioned serum-free stem cell growth medium with additional supplements, including 100 ng/mL recombinant human platelet-derived growth factor-AA, 25 μg/mL insulin, 100 μg/mL transferrin, 15 μM putrescine, 30 nM selenite, 2 μg/mL heparan sulfate, 0.9% glucose, 4 mM L-glutamine, and 20 nM progesterone. To measure antiproliferative activity, 2000 cells/well were seeded into 96-well plates and treated with 0.002, 0.02, 0.2, 2, and 20 μM of the selected compounds in 100 μL of culture medium for up to 13 days. Cell viability was measured at days 4, 7, 10, and 13 by Cell Counting Kit-8 (Dojindo Molecular Technologies, Rockville, MD) according to the manufacturer's instructions as we described previously.^{31,35}

■ ASSOCIATED CONTENT

§ Supporting Information

Alignments of crystal structures of IDH1 forms bound to substrates and inhibitors and experimental procedures providing details of compound synthesis and characterization. This material is available free of charge via the Internet at <http://pubs.acs.org>.

■ AUTHOR INFORMATION

Corresponding Author

*Tel: 713-798-7415. E-mail: ysong@bcm.edu.

Author Contributions

[¶]Z.L. and Y.Y. contributed equally.

Notes

The authors declare no competing financial interest.

■ ACKNOWLEDGMENTS

This work was supported by a grant (R01NS080963) from National Institute of Neurological Disorders and Stroke (NINDS/NIH) and a grant (RP140469) from Cancer Prevention and Research Institute of Texas (CPRIT) to Y.S., as well as a grant (R01CA127963) to J.M.G.

■ ABBREVIATIONS

α-KG, α-ketoglutaric acid; BBB, blood–brain barrier; D2HG, D-2-hydroxyglutaric acid; ICT, isocitric acid; IDH, isocitrate hydrogenase; MDR1, multidrug resistance 1; R132H, Arg132 mutation to His; R132C, Arg132 mutation to Cys; SAR, structure–activity relationship; WT, wild-type

■ REFERENCES

- (1) Xu, X.; Zhao, J.; Xu, Z.; Peng, B.; Huang, Q.; Arnold, E.; Ding, J. Structures of human cytosolic NADP-dependent isocitrate dehydrogenase reveal a novel self-regulatory mechanism of activity. *J. Biol. Chem.* **2004**, *279*, 33946–33957.
- (2) Haselbeck, R. J.; McAlister-Henn, L. Function and expression of yeast mitochondrial NAD- and NADP-specific isocitrate dehydrogenases. *J. Biol. Chem.* **1993**, *268*, 12116–12122.
- (3) Jennings, G. T.; Sechi, S.; Stevenson, P. M.; Tuckey, R. C.; Parmelee, D.; McAlister-Henn, L. Cytosolic NADP(+)-dependent isocitrate dehydrogenase. Isolation of rat cDNA and study of tissue-specific and developmental expression of mRNA. *J. Biol. Chem.* **1994**, *269*, 23128–23134.
- (4) Parsons, D. W.; Jones, S.; Zhang, X.; Lin, J. C.; Leary, R. J.; Angenendt, P.; Mankoo, P.; Carter, H.; Siu, I. M.; Gallia, G. L.; Olivieri, A.; McLendon, R.; Rasheed, B. A.; Keir, S.; Nikolskaya, T.; Nikolsky, Y.; Busam, D. A.; Tekleab, H.; Diaz, L. A., Jr.; Hartigan, J.; Smith, D. R.; Strausberg, R. L.; Marie, S. K.; Shinjo, S. M.; Yan, H.; Riggins, G. J.; Bigner, D. D.; Karchin, R.; Papadopoulos, N.; Parmigiani, G.; Vogelstein, B.; Velculescu, V. E.; Kinzler, K. W. An integrated genomic analysis of human glioblastoma multiforme. *Science* **2008**, *321*, 1807–1812.
- (5) Xu, W.; Yang, H.; Liu, Y.; Yang, Y.; Wang, P.; Kim, S. H.; Ito, S.; Yang, C.; Xiao, M. T.; Liu, L. X.; Jiang, W. Q.; Liu, J.; Zhang, J. Y.; Wang, B.; Frye, S.; Zhang, Y.; Xu, Y. H.; Lei, Q. Y.; Guan, K. L.; Zhao, S. M.; Xiong, Y. Oncometabolite 2-hydroxyglutarate is a competitive inhibitor of alpha-ketoglutarate-dependent dioxygenases. *Cancer Cell* **2011**, *19*, 17–30.
- (6) Gross, S.; Cairns, R. A.; Minden, M. D.; Driggers, E. M.; Bittinger, M. A.; Jang, H. G.; Sasaki, M.; Jin, S.; Schenkein, D. P.; Su, S. M.; Dang, L.; Fantin, V. R.; Mak, T. W. Cancer-associated metabolite 2-hydroxyglutarate accumulates in acute myelogenous leukemia with isocitrate dehydrogenase 1 and 2 mutations. *J. Exp. Med.* **2010**, *207*, 339–344.

- (7) Yan, H.; Parsons, D. W.; Jin, G.; McLendon, R.; Rasheed, B. A.; Yuan, W.; Kos, I.; Batinic-Haberle, I.; Jones, S.; Riggins, G. J.; Friedman, H.; Friedman, A.; Reardon, D.; Herndon, J.; Kinzler, K. W.; Velculescu, V. E.; Vogelstein, B.; Bigner, D. D. IDH1 and IDH2 mutations in gliomas. *N. Engl. J. Med.* **2009**, *360*, 765–773.
- (8) Hartmann, C.; Meyer, J.; Bals, J.; Capper, D.; Mueller, W.; Christians, A.; Felsberg, J.; Wolter, M.; Mawrin, C.; Wick, W.; Weller, M.; Herold-Mende, C.; Unterberg, A.; Jeuken, J. W.; Wesseling, P.; Reifenberger, G.; von Deimling, A. Type and frequency of IDH1 and IDH2 mutations are related to astrocytic and oligodendroglial differentiation and age: A study of 1,010 diffuse gliomas. *Acta Neuropathol.* **2009**, *118*, 469–474.
- (9) Marcucci, G.; Maharry, K.; Wu, Y.-Z.; Radmacher, M. D.; Mrózek, K.; Margeson, D.; Holland, K. B.; Whitman, S. P.; Becker, H.; Schwind, S.; Metzeler, K. H.; Powell, B. L.; Carter, T. H.; Kollitz, J. E.; Wetzler, M.; Carroll, A. J.; Baer, M. R.; Caligiuri, M. A.; Larson, R. A.; Bloomfield, C. D. IDH1 and IDH2 gene mutations identify novel molecular subsets within de novo cytogenetically normal acute myeloid leukemia: A cancer and leukemia group B study. *J. Clin. Oncol.* **2010**, *28*, 2348–2355.
- (10) Figueroa, M. E.; Abdel-Wahab, O.; Lu, C.; Ward, P. S.; Patel, J.; Shih, A.; Li, Y.; Bhagwat, N.; Vasanthakumar, A.; Fernandez, H. F.; Tallman, M. S.; Sun, Z.; Wolniak, K.; Peeters, J. K.; Liu, W.; Choe, S. E.; Fantin, V. R.; Paietta, E.; Löwenberg, B.; Licht, J. D.; Godley, L. A.; Delwel, R.; Valk, P. J.; Thompson, C. B.; Levine, R. L.; Melnick, A. Leukemic IDH1 and IDH2 mutations result in a hypermethylation phenotype, disrupt TET2 function, and impair hematopoietic differentiation. *Cancer Cell* **2010**, *18*, 553–567.
- (11) Amary, M. F.; Bacs, K.; Maggiani, F.; Damato, S.; Halai, D.; Berisha, F.; Pollock, R.; O'Donnell, P.; Grigoriadis, A.; Diss, T.; Eskandarpour, M.; Presneau, N.; Hogendoorn, P. C.; Futreal, A.; Tirabosco, R.; Flanagan, A. M. IDH1 and IDH2 mutations are frequent events in central chondrosarcoma and central and periosteal chondromas but not in other mesenchymal tumours. *J. Pathol.* **2011**, *224*, 334–343.
- (12) Dang, L.; White, D. W.; Gross, S.; Bennett, B. D.; Bittinger, M. A.; Driggers, E. M.; Fantin, V. R.; Jang, H. G.; Jin, S.; Keenan, M. C.; Marks, K. M.; Prins, R. M.; Ward, P. S.; Yen, K. E.; Liao, L. M.; Rabinowitz, J. D.; Cantley, L. C.; Thompson, C. B.; van der Heiden, M. G.; Su, S. M. Cancer-associated IDH1 mutations produce 2-hydroxyglutarate. *Nature* **2009**, *462*, 739–744.
- (13) Ward, P. S.; Patel, J.; Wise, D. R.; Abdel-Wahab, O.; Bennett, B. D.; Collier, H. A.; Cross, J. R.; Fantin, V. R.; Hedvat, C. V.; Perl, A. E.; Rabinowitz, J. D.; Carroll, M.; Su, S. M.; Sharp, K. A.; Levine, R. L.; Thompson, C. B. The common feature of leukemia-associated IDH1 and IDH2 mutations is a neomorphic enzyme activity converting alpha-ketoglutarate to 2-hydroxyglutarate. *Cancer Cell* **2010**, *17*, 225–234.
- (14) Lu, C.; Ward, P. S.; Kapoor, G. S.; Rohle, D.; Turcan, S.; Abdel-Wahab, O.; Edwards, C. R.; Khanin, R.; Figueroa, M. E.; Melnick, A.; Wellen, K. E.; O'Rourke, D. M.; Berger, S. L.; Chan, T. A.; Levine, R. L.; Mellinghoff, I. K.; Thompson, C. B. IDH1 mutation impairs histone demethylation and results in a block to cell differentiation. *Nature* **2012**, *483*, 474–478.
- (15) Turcan, S.; Rohle, D.; Goenka, A.; Walsh, L. A.; Fang, F.; Yilmaz, E.; Campos, C.; Fabius, A. W.; Lu, C.; Ward, P. S.; Thompson, C. B.; Kaufman, A.; Guryanova, O.; Levine, R.; Heguy, A.; Viale, A.; Morris, L. G.; Huse, J. T.; Mellinghoff, I. K.; Chan, T. A. IDH1 mutation is sufficient to establish the glioma hypermethylator phenotype. *Nature* **2012**, *483*, 479–483.
- (16) Prensner, J. R.; Chinnaiyan, A. M. Metabolism unhinged: IDH mutations in cancer. *Nat. Med.* **2011**, *17*, 291–293.
- (17) Dang, L.; Jin, S.; Su, S. M. IDH mutations in glioma and acute myeloid leukemia. *Trends Mol. Med.* **2010**, *16*, 387–397.
- (18) Garber, K. Oncometabolite? IDH1 discoveries raise possibility of new metabolism targets in brain cancers and leukemia. *J. Natl. Cancer Inst.* **2010**, *102*, 926–928.
- (19) Popovici-Muller, J.; Saunders, J. O.; Salituro, F. G.; Travins, J. M.; Yan, S.; Zhao, F.; Gross, S.; Dang, L.; Yen, K. E.; Yang, H.; Straley, K. S.; Jin, S.; Kunii, K.; Fantin, V. R.; Zhang, S.; Pan, Q.; Shi, D.; Biller, S. A.; Su, S. M. Discovery of the first potent inhibitors of mutant IDH1 that lower tumor 2-HG in vivo. *ACS Med. Chem. Lett.* **2012**, *3*, 850–855.
- (20) Rohle, D.; Popovici-Muller, J.; Palaskas, N.; Turcan, S.; Grommes, C.; Campos, C.; Tsoi, J.; Clark, O.; Oldrini, B.; Komisopoulou, E.; Kunii, K.; Pedraza, A.; Schalm, S.; Silverman, L.; Miller, A.; Wang, F.; Yang, H.; Chen, Y.; Kernytsky, A.; Rosenblum, M. K.; Liu, W.; Biller, S. A.; Su, S. M.; Brennan, C. W.; Chan, T. A.; Graeber, T. G.; Yen, K. E.; Mellinghoff, I. K. An inhibitor of mutant IDH1 delays growth and promotes differentiation of glioma cells. *Science* **2013**, *340*, 626–630.
- (21) Zheng, B.; Yao, Y.; Liu, Z.; Deng, L.; Anglin, J. L.; Jiang, H.; Prasad, B. V.; Song, Y. Crystallographic Investigation and Selective Inhibition of Mutant Isocitrate Dehydrogenase. *ACS Med. Chem. Lett.* **2013**, *4*, 542–546.
- (22) Deng, L.; Sundriyal, S.; Rubio, V.; Shi, Z.; Song, Y. Coordination chemistry based approach to lipophilic inhibitors of 1-deoxy-D-xylulose-5-phosphate reductoisomerase. *J. Med. Chem.* **2009**, *52*, 6539–6542.
- (23) Deng, L.; Endo, K.; Kato, M.; Cheng, G.; Yajima, S.; Song, Y. Structures of 1-Deoxy-D-Xylulose-5-Phosphate Reductoisomerase/Lipophilic Phosphonate Complexes. *ACS Med. Chem. Lett.* **2011**, *2*, 165–170.
- (24) Xue, J.; Diao, J.; Cai, G.; Deng, L.; Zheng, B.; Yao, Y.; Song, Y. Antimalarial and Structural Studies of Pyridine-containing Inhibitors of 1-Deoxyxylulose-5-phosphate Reductoisomerase. *ACS Med. Chem. Lett.* **2013**, *4*, 278–282.
- (25) Yang, B.; Zhong, C.; Peng, Y.; Lai, Z.; Ding, J. Molecular mechanisms of “off-on switch” of activities of human IDH1 by tumor-associated mutation R132H. *Cell Res.* **2010**, *20*, 1188–1200.
- (26) Jin, G.; Pirozzi, C. J.; Chen, L. H.; Lopez, G. Y.; Duncan, C. G.; Feng, J.; Spasojevic, I.; Bigner, D. D.; He, Y.; Yan, H. Mutant IDH1 is required for IDH1 mutated tumor cell growth. *Oncotarget* **2012**, *3*, 774–782.
- (27) Hellinger, E.; Veszelka, S.; Toth, A. E.; Walter, F.; Kittel, A.; Bak, M. L.; Tihanyi, K.; Hada, V.; Nakagawa, S.; Duy, T. D.; Niwa, M.; Deli, M. A.; Vastag, M. Comparison of brain capillary endothelial cell-based and epithelial (MDCK-MDR1, Caco-2, and VB-Caco-2) cell-based surrogate blood-brain barrier penetration models. *Eur. J. Pharm. Biopharm.* **2012**, *82*, 340–351.
- (28) Lv, H.; Zhang, X.; Sharma, J.; Reddy, M. V. R.; Reddy, E. P.; Gallo, J. M. Integrated pharmacokinetic-driven approach to screen candidate anticancer drugs for brain tumor chemotherapy. *AAPS J.* **2013**, *15*, 250–257.
- (29) Luchman, H. A.; Stechishin, O. D.; Dang, N. H.; Blough, M. D.; Chesnelong, C.; Kelly, J. J.; Nguyen, S. A.; Chan, J. A.; Weljie, A. M.; Cairncross, J. G.; Weiss, S. An in vivo patient-derived model of endogenous IDH1-mutant glioma. *Neuro-Oncology* **2012**, *14*, 184–191.
- (30) Shu, Q.; Wong, K. K.; Su, J. M.; Adesina, A. M.; Yu, L. T.; Tsang, Y. T.; Antalfy, B. C.; Baxter, P.; Perlaky, L.; Yang, J.; Dauser, R. C.; Chintagumpala, M.; Blaney, S. M.; Lau, C. C.; Li, X. N. Direct orthotopic transplantation of fresh surgical specimen preserves CD133+ tumor cells in clinically relevant mouse models of medulloblastoma and glioma. *Stem Cells* **2008**, *26*, 1414–1424.
- (31) Liu, Z.; Zhao, X.; Mao, H.; Baxter, P. A.; Huang, Y.; Yu, L.; Wadhwa, L.; Su, J. M.; Adesina, A.; Perlaky, L.; Hurwitz, M.; Idamakanti, N.; Police, S. R.; Hallenbeck, P. L.; Hurwitz, R. L.; Lau, C. C.; Chintagumpala, M.; Blaney, S. M.; Li, X. N. Intravenous injection of oncolytic picornavirus SVV-001 prolongs animal survival in a panel of primary tumor-based orthotopic xenograft mouse models of pediatric glioma. *Neuro-Oncology* **2013**, *15*, 1173–1185.
- (32) Wan, F.; Zhang, S.; Xie, R.; Gao, B.; Campos, B.; Herold-Mende, C.; Lei, T. The utility and limitations of neurosphere assay, CD133 immunophenotyping and side population assay in glioma stem cell research. *Brain Pathol.* **2010**, *20*, 877–889.
- (33) Laks, D. R.; Masterman-Smith, M.; Visnyei, K.; Angenieux, B.; Orozco, N. M.; Foran, I.; Yong, W. H.; Vinters, H. V.; Liao, L. M.;

Lazareff, J. A.; Mischel, P. S.; Cloughesy, T. F.; Horvath, S.; Kornblum, H. I. Neurosphere formation is an independent predictor of clinical outcome in malignant glioma. *Stem Cells* **2009**, *27*, 980–987.

(34) Chaichana, K.; Zamora-Berridi, G.; Camara-Quintana, J.; Quinones-Hinojosa, A. Neurosphere assays: Growth factors and hormone differences in tumor and nontumor studies. *Stem Cells* **2006**, *24*, 2851–2857.

(35) Yu, L.; Baxter, P. A.; Voicu, H.; Gurusiddappa, S.; Zhao, Y.; Adesina, A.; Man, T. K.; Shu, Q.; Zhang, Y. J.; Zhao, X. M.; Su, J. M.; Perlaky, L.; Dauser, R.; Chintagumpala, M.; Lau, C. C.; Blaney, S. M.; Rao, P. H.; Leung, H. C.; Li, X. N. A clinically relevant orthotopic xenograft model of ependymoma that maintains the genomic signature of the primary tumor and preserves cancer stem cells in vivo. *Neuro-Oncology* **2010**, *12*, 580–594.

(36) Lapidot, T.; Sirard, C.; Vormoor, J.; Murdoch, B.; Hoang, T.; Caceres-Cortes, J.; Minden, M.; Paterson, B.; Caligiuri, M. A.; Dick, J. E. A cell initiating human acute myeloid leukaemia after transplantation into SCID mice. *Nature* **1994**, *367*, 645–648.

(37) Al Hajj, M.; Becker, M. W.; Wicha, M.; Weissman, I.; Clarke, M. F. Therapeutic implications of cancer stem cells. *Curr. Opin. Genet. Dev.* **2004**, *14*, 43–47.

(38) Zhou, H.; Shen, T.; Luo, Y.; Liu, L.; Chen, W.; Xu, B.; Han, X.; Pang, J.; Rivera, C. A.; Huang, S. The antitumor activity of the fungicide ciclopirox. *Int. J. Cancer* **2010**, *127*, 2467–2477.

(39) Eberhard, Y.; McDermott, S. P.; Wang, X.; Gronda, M.; Venugopal, A.; Wood, T. E.; Hurren, R.; Datti, A.; Batey, R. A.; Wrana, J.; Antholine, W. E.; Dick, J. E.; Schimmer, A. D. *Blood* **2009**, *114*, 3064–3073.

(40) Deodhar, K. D.; Kekare, M. B.; Pednekar, S. R. A Facile Synthesis of 2-Pyridones by Nucleophilic Reaction on Pyran2-thiones. *Synthesis* **1985**, 328–331.

(41) Batt, D. G.; Maynard, G. D.; Petraitis, J. J.; Shaw, J. E.; Galbraith, W.; Harris, R. R. 2-Substituted-1-naphthols as potent 5-lipoxygenase inhibitors with topical antiinflammatory activity. *J. Med. Chem.* **1990**, *33*, 360–370.